PHYSICAL REVIEW B VOLUME 19, NUMBER 8 15 APRIL 1979

Molecular dynamics of shock waves in one-dimensional chains. II. Thermalization

G. K. Straub and B. L. Holian
Los Alamos Scientific Laboratory, Los Alamos, New Mexico 87544

R. G. Petschek
Harvard University, Cambridge, Massachusetts 02138

(Received 13 November 1978)

The thermalization behavior behind a shock front in one-dimensional chains has been studied in a series of molecular-dynamics computer experiments. We have found that a shock wave generated in a chain initially at finite temperature has essentially the same characteristics as in a chain initially at zero temperature. We also find that the final velocity distribution function for particles behind the shock front is not the Maxwell-Boltzmann distribution for an equilibrium system of classical particles. For times long after the shock has passed, we propose a nonequilibrium velocity distribution which is based upon behavior in the harmonic and hard-rod limits and agrees with our numerical results. Temperature profiles for both harmonic and anharmonic chains are found to exhibit a long-time tail that decays inversely with time. Finally, we have run a computer experiment to generate what qualitatively resembles solitons in Toda chains by means of shock waves.

I. INTRODUCTION

In a previous paper, we gave the results of molecular-dynamics calculations of shock waves in one-dimensional chains, including a brief description of the effect of a finite initial temperature.[1] We found that a shock wave generated in a chain initially at finite temperature has essentially the same characteristics as in a chain initially at zero temperature. At about the same time, other investigators reported calculations which they interpreted as showing that thermal equilibrium behind the shock front was approached provided that the chain was initially at some finite temperature rather than at zero initial temperature.[2] Upon examination of their results and after additional calculations of our own, we have found that, quite the contrary, no thermal equilibration occurs behind the shock front for strong shocks in one-dimensional chains, whether the initial temperature is zero or finite.

Throughout this paper, we use the term "thermal equilibrium" to mean that a classical system of particles in thermal equilibrium has a Maxwell-Boltzmann (or Gaussian) velocity distribution. This definition is restrictive in the sense that nonequilibrium systems include steady-state systems where rates or gradients are non-negligible as well as transient, or time-dependent systems. Although our initial velocity distributions are Maxwellian, we observe final distributions behind shock fronts that are not. In particular, if there is a final temperature rise as in the case of a strong shock, then there is no thermal equilibration, even though the temperature has reached a steady-state value. For times long after the shock has passed, we propose a nonequilibrium velocity distribution, which is based upon behavior in the harmonic and hard-rod limits, and which agrees with molecular-dynamics results for various shock strengths and initial temperatures.

In Sec. II, we give a brief review of the molecular-dynamics method and the boundary conditions we have used to generate a shock wave in a thermalized chain. We also show that shock strength scaling by αv (α is the cubic anharmonicity coefficient and $v = u_p/c_0$ is the particle velocity u_p divided by the long-wavelength sound speed c_0) is generally applicable for pair potentials characterized by either two or three parameters such as energy and distance scales and the anharmonicity coefficient.

In Sec. III, we present the results of our study. The temperature rise ϵ behind the shock is calculated as a function of αv for the Toda chain as well as the thermal relaxation time (shock thickness) $\tau_{1/2}(n)$, which is the time required for the temperature in the region around particle n to decay from the initial response halfway down to the final value ($\tau_{1/2}$ is proportional to n for shock waves in anharmonic chains). Both the temperature rise and thermal relaxation time are found not to be strongly affected by the initial temperature. A surprising result is that while the fractional thermal shock thickness decreases with shock strength αv beyond $\alpha v = 1$ (the onset of steady-wave behavior), the departure of the velocity distribution from Maxwellian increases with αv.

We have also found that the temperature profiles for both harmonic and anharmonic chains exhibit a long-time tail. Following excitation by the

shock front, the initial decay is approximately exponential; thereafter the decay is inversely proportional to time.

A computer experiment to generate what qualitatively resembles solitons in Toda chains by means of shock waves is discussed. We observe many closely spaced, nearly-equal-amplitude solitary waves whose velocities are proportional to amplitude and which apparently remain unchanged after collisions.

II. REVIEW OF METHODS

The molecular-dynamics method for nearest-neighbor one-dimensional chains was outlined in Ref. 1 and will be only briefly reviewed here. Consider a chain of N particles (particle number $n=1,2,\ldots,N$) each of mass m, the unit of mass. The displacement of particle n, x_n, is given in units of the lattice spacing a, and time t is given in units of $1/\omega_0$, where ω_0 is the fundamental harmonic frequency given by $m\omega_0^2=\phi''(0)$, the second spatial derivative of the pair potential evaluated at zero relative displacement of particles. The equations of motion are given by

$$\begin{aligned}\ddot{x}_n(t) &= \phi'(x_{n+1,n}) - \phi'(x_{n,n-1}) \\ &= x_{n+1,n} - x_{n,n-1} - \alpha(x_{n+1,n}^2 - x_{n,n-1}^2) \\ &\quad + \beta(x_{n+1,n}^3 - x_{n,n-1}^3) + \cdots, \end{aligned} \tag{1}$$

where primes indicate spatial derivatives, dots indicate time derivatives, $x_{ij}=x_i-x_j$ is the relative displacement of nearest neighbors i and j, α is the cubic anharmonicity coefficient $\alpha = -a\phi'''(0)/2\phi''(0)$, and β is the quartic anharmonicity coefficient $\beta = a^2\phi''''(0)/6\phi''(0)$.

The unit of velocity in this system is $c_0=a\omega_0$, the long-wavelength harmonic sound speed, and the unit of energy is mc_0^2.

The nearest-neighbor Toda potential

$$\phi(x_{ij}) = (1/4\alpha^2)[\exp(-2\alpha x_{ij}) + 2\alpha x_{ij} - 1] \tag{2}$$

was used throughout, except for one comparison calculation using the nearest-neighbor Morse potential

$$\phi(x_{ij}) = (9/8\alpha^2)[\exp(-\tfrac{2}{3}\alpha x_{ij}) - 1]^2. \tag{3}$$

Both potentials are expressed in units of mc_0^2 with relative displacements scaled by a. The third parameter in these potentials allows one to vary the anharmonicity α from zero (the harmonic limit) to infinity (the hard-rod limit).

If the displacements x_n in Eq. (1) are further divided by v (reduced particle velocity), so that velocities are now expressed in units of particle velocity u_p and energies in units of mu_p^2, then Eqs. (1)–(3) are unchanged except to replace α by αv, β by βv^2, etc. For a three-parameter potential such as Toda or Morse, α and v appear only as the product αv in the equations of motion and the potential, so that αv uniquely scales the shock strength. Obviously, a two-parameter potential such as Lennard-Jones 6-12 has a fixed anharmonicity so that v by itself characterizes shock strength. This scaling no longer holds for potentials with four or more parameters; for example, shock waves in chains of particles interacting via the truncated quartic potential with $\alpha=0,\beta>0$ are characterized by βv^2 and not αv.

In order to reduce surface (end) effects in thermalized chains, that is, to minimize the inward propagation of thermal expansion waves into the chain, we impose periodic boundary conditions during equilibration to the initial temperature and then shrink the periodic length during the shock process ($t>0$) according to $L(t)=Na-2u_pt$. A right-running shock wave proceeds from the left boundary while a left-running shock travels from the right boundary, thus closely mocking up a symmetric-impact flying-plate shock-wave experiment. Until these shock waves collide in the middle of the chain, the results for particles far enough from either periodic boundary are the same as for the piston-particle scheme.[1] The time step Δt for the central-difference approximation to the equations of motion was chosen for weak shocks ($\alpha v \lesssim \frac{1}{2}$) to be about $\frac{1}{60}$ of the fundamental period of vibration and reduced in proportion to αv for stronger shocks.

Equilibration to an initial temperature is achieved in the standard way: particles are started at lattice sites with random velocities chosen according to the harmonic equipartitioning of kinetic and potential energies, and such that there is no residual center-of-mass motion. Typically, 40–50 fundamental periods are allowed to achieve a random configuration before the shock process is begun.

Time and spatial averages of the temperature (second-order cumulant, or variance, of the velocity) and kurtosis (fourth-order cumulant of the velocity) were computed over at least one fundamental period in time and 25 particles. The reduced temperature at time t and particle n is defined to be (k_B is Boltzmann's constant)

$$\begin{aligned}\mathcal{T}_n(t) &= k_B T_n(t)/mu_p^2 \\ &= \langle(v-\langle v\rangle)^2\rangle/u_p^2 \\ &= (\langle v^2\rangle - \langle v\rangle^2)/u_p^2, \end{aligned} \tag{4}$$

where $v=\dot{x}$ is the velocity, and velocity moments are computed according to

$$\langle v^k\rangle = (2l+1)^{-1}\sum_{i=n-l}^{n+l}(m)^{-1}\sum_{j=1}^{m} v_i^k[t-(m-j)\Delta t]. \tag{5}$$

Lagrangian coordinate n and time t are implicit in the angular brackets. The number of time steps in the average is m and the number of particles in the average is $2l+1$. The reduced kurtosis at time t and particle n is defined to be

$$\begin{aligned}\mathcal{C}_n(t) &= \langle (v-\langle v\rangle)^4\rangle/u_p^4 - 3\mathcal{T}_n^2(t)\\ &= (\langle v^4\rangle - 4\langle v^3\rangle\langle v\rangle + 12\langle v^2\rangle\langle v\rangle^2\\ &\quad - 3\langle v^2\rangle^2 - 6\langle v\rangle^4)/u_p^4. \end{aligned} \tag{6}$$

If the velocity distribution is Maxwellian (Gaussian), then the kurtosis and all higher-order cumulants are zero. The multiplicative correction factors for finite sample size, to first order, can be shown to be $1+(2l+1)^{-1}$ for the temperature and $1+6(2l+1)^{-1}$ for the kurtosis.

III. RESULTS AND DISCUSSION

As the shock wave travels down the chain, we denote the time for the initial peak temperature of particle n as $t_n^{(1)}$ and the time required for the temperature to decay halfway down to its final value as $\tau_{1/2}(n)$. The final temperature rise behind the shock front is

$$\epsilon = \mathcal{T} - \mathcal{T}_0, \tag{7}$$

where the final temperature $\mathcal{T}$ and initial temperature $\mathcal{T}_0$ are time and spatial averages of $\mathcal{T}_n(t)$ behind and ahead of the shock front, respectively. In Fig. 1, ϵ and the coefficient of proportionality of the thermal relaxation time $\tau_{1/2}(n)$ to particle number n are presented as functions of the shock strength $\alpha\nu$ for $\mathcal{T}_0=0$. In the harmonic limit, the thermal relaxation time is proportional to $n^{1/3}$, so that the shock thickness is a continually decreasing fraction of shocked material. In anharmonic chains, the shock thickness is a constant fraction of the number of shocked particles. From Fig. 1 it is apparent that as the hard-rod limit is approached ($\alpha\nu\to\infty$), the fractional shock thickness again approaches zero. The maximum fractional shock thickness occurs near $\alpha\nu=1$, i.e., near the onset of steady-wave (hard-rod-like) behavior.[1] For comparison the parameter $\tilde{\epsilon}$, defined in Ref. 1 as the square of the maximum steady-wave velocity amplitude at long times,

$$\tilde{\epsilon} = \lim_{t\to\infty} \max[v_n(t)/u_p - 1]^2 \quad \text{for } n \gg 1 \tag{8}$$

is also plotted. $\tilde{\epsilon}$ is larger than ϵ by virtue of the fact that the steady velocity waves are not perfect hard-rod square waves until $\alpha\nu\to\infty$, where $\tilde{\epsilon}=\epsilon$. The most notable difference between the $\mathcal{T}_0=0$ data of Fig. 1 and the results for $\mathcal{T}_0>0$ is a slight rise in final temperature for weak shocks ($\alpha\nu<1$), which is at most $\epsilon\sim 0.05$. Also, for strong shocks in very-high-temperature chains (such as $\alpha\nu = 5.25$, $\mathcal{T}_0=0.12$) the shock thickness is almost twice that of the $\mathcal{T}_0=0$ case. A summary of calculations is presented in Table I.

After an exponential decay from the initial peak response at time $t_n^{(1)}$ for particle n, the temperature profile for $t \gg t_n^{(1)} + \tau_{1/2}(n)$ decays very slowly to its final value. It can be shown[1] that in the harmonic limit, for time $t \gg n \gg 1$,

$$\begin{aligned}\mathcal{T}_n(t) &\sim \frac{1}{2\pi}\int_{t-2\pi}^{t} dt' \left(\frac{v_n(t')}{u_p} - 1\right)^2\\ &\sim \frac{1}{2\pi}\int_{t-2\pi}^{t} dt' J_{2n}^2(2t')\\ &\sim \frac{1}{2\pi}\int_{t-2\pi}^{t} dt' \frac{\cos^2(2t' - n\pi - \frac{1}{4}\pi)}{\pi t'}\\ &\sim \frac{1}{2\pi t}, \end{aligned} \tag{9}$$

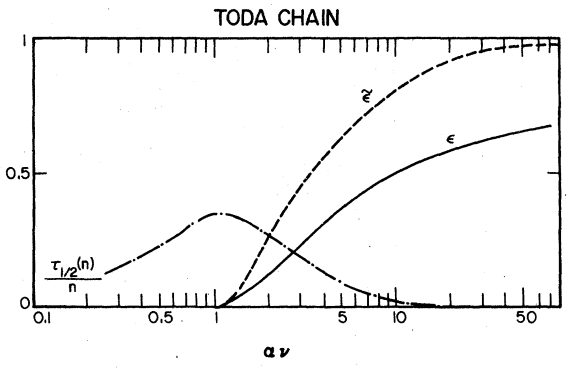

FIG. 1. Temperature rise ϵ behind the shock front and the proportionality of the thermal relaxation time to particle number ($n \gg 1$), $\tau_{1/2}(n)/n$, vs shock strength $\alpha\nu$ in initially quiescent ($\mathcal{T}_0=0$) Toda chains. $\tilde{\epsilon}$ is the square of the long-time steady-wave velocity amplitude [see Eq. (8)].

TABLE I. Shock waves in Toda chains. Thermalization parameters as functions of the shock strength $\alpha\nu$: $\mathcal{T}_0 = k_B T_0/mu_p^2$ is the initial temperature, $\mathcal{T}$ is the final temperature, $\mathcal{C}$ is the kurtosis, $\tau_{1/2}$ is the thermal relaxation time, and A_n is the coefficient of the long-time tail of the temperature profile (for particle number $n \gg 1$).

$\alpha\nu$	$\mathcal{T}_0$	$\mathcal{T}-\mathcal{T}_0$	$(-\frac{1}{2}\mathcal{C})^{1/2}$	$\tau_{1/2}(n)/n$	A_n [a]
0.0	0.0	0.0	0.0	0.0	0.16
0.3	0.0	0.0	0.0	0.15	0.21
0.3	0.25	0.05	0.05	0.17	···
0.525	0.0	0.0	0.0	0.23	0.28
0.525	0.1	0.05	0.05	0.23	···
1.05	0.0	0.0011	~0.0	0.35	1.09
3.0	0.0	0.23	0.23	0.18	···
5.25	0.0	0.37	0.36	0.09	···
5.25	0.001	0.37	0.36	0.09	···
5.25	0.12	0.38	0.38	0.17	···
52.5	0.0	0.65	0.65	0.0	···

[a] For $\alpha\nu = 0$, $\mathcal{T}_n \to \mathcal{T} + A/t$; for $\alpha\nu > 0$, $\mathcal{T}_n \to \mathcal{T} + A_n/(t - t_n^{(1)})$, where $t_n^{(1)}$ is the time of the first peak in the temperature profile.

where J_{2n} is the Bessel function of the first kind of order $2n$. The molecular-dynamics result for $t\mathcal{T}_n(t)$ is 0.163 compared with the theoretical value from Eq. (9), $1/2\pi = 0.159$ ($t = 1000, n = 113$). The calculated profile for $n = 13$ and $t \sim 1000$ is characterized by oscillations of frequency $\omega(t \to \infty)/\omega_0 = 2.01$, compared to the theoretical[1] value of 2, and amplitude 0.0175, compared to the theoretical value $(\pi t)^{-1/2} = 0.0178$. The same qualitative long-time tail (t^{-1}) is found for anharmonic chains, though the following form including the temperature rise appears to fit the data better ($t \gg t_n^{(1)}$, $n \gg 1$):

$$\mathcal{T}_n(t) \sim \mathcal{T} + A_n/(t - t_n^{(1)}). \tag{10}$$

We have used this formula to verify that steady-wave behavior begins very near $\alpha\nu = 1$ in Toda chains: at $\alpha\nu = 1.05$, temperature profiles were fitted with $\epsilon = 0.0011 \pm 0.0002$. In the hard-rod limit, A_n will go to zero. Comparing the behavior of A_n and the thermal relaxation proportionality constant $\tau_{1/2}(n)/n$, one sees that both quantities reach some maximum value for increasing $\alpha\nu$ and then return to zero. Since the calculation of A_n becomes difficult much beyond $\alpha\nu = 1$, once ϵ becomes appreciable, one cannot determine if both maxima occur for the same value of $\alpha\nu$.

The velocity distribution function far behind the shock front is of special interest to us, since we can characterize the thermalization process by comparing this distribution function and its cumulants to the Maxwell-Boltzmann (or Gaussian) velocity distribution for a thermally equilibrated classical system. Consider a symmetric-impact flying-plate shock-wave experiment where two zero-temperature semi-infinite hard-rod chains are rushing toward each other, the left-hand chain at velocity $v = +1$ (in units of u_p) and the right-hand chain at velocity $v = -1$. The initial velocity distribution is the sum of two Dirac δ functions, one centered at $v = +1$ for the left-hand side and the other at $v = -1$ for the right-hand side. Since hard rods of equal mass exchange velocities upon collision, the final velocity distribution behind the two shock fronts is unchanged from the initial one. A similar result is obtained if each side is initially equilibrated at the same finite initial temperature, $\mathcal{T}_0 > 0$. In this case, the sum of two Gaussian velocity distributions, with width appropriate to $\mathcal{T}_0$ and centered at $v = \pm 1$, remains unchanged behind the outward-advancing shock fronts. In both cases, the final temperature $\mathcal{T}$ behind the shock is higher than the initial temperature by the amount $\epsilon = \mathcal{T} - \mathcal{T}_0 = 1$.

If we repeat this experiment with two zero-temperature semi-infinite harmonic chains, the final velocity distribution behind the shock fronts will be different from the initial distribution; that is, it will be a single Dirac δ function centered at $v = 0$ with no temperature rise: $\epsilon = \mathcal{T} - \mathcal{T}_0 = 0$. This result is likewise obtained for weak shocks ($\alpha\nu < 1$, $\epsilon = 0$) in zero-temperature anharmonic chains.

In order to generalize these results for finite initial temperature and any shock strength, we propose the following model for the final velocity distribution behind a shock wave in a one-dimensional chain—the "ϵ distribution":

$$f_\epsilon(v) = \tfrac{1}{2}(2\pi\mathcal{T}_0)^{-1/2} \times\left[\exp\left(-\frac{(v-\epsilon^{1/2})^2}{2\mathcal{T}_0}\right) + \exp\left(-\frac{(v+\epsilon^{1/2})^2}{2\mathcal{T}_0}\right)\right]. \tag{11}$$

In the hard-rod limit, $\alpha\nu \to \infty$ and $\epsilon \to 1$, so that

$$f_\epsilon(v) \to f_1(v) = \tfrac{1}{2}(2\pi\mathcal{T}_0)^{-1/2} \times\left[\exp\left(-\frac{(v-1)^2}{2\mathcal{T}_0}\right) + \exp\left(\frac{(v+1)^2}{2\mathcal{T}_0}\right)\right]. \tag{12}$$

At $\mathcal{T}_0 = 0$, Eq. (12) becomes

$$f_1(v) = \tfrac{1}{2}[\delta(v-1) + \delta(v+1)]. \tag{13}$$

In the harmonic limit, $\alpha\nu \to 0$ and $\epsilon \to 0$, so that

$$f_\epsilon(v) \to f_0(v) = (2\pi\mathcal{T}_0)^{-1/2}\exp(-v^2/2\mathcal{T}_0), \tag{14}$$

the Maxwellian (Gaussian) velocity distribution. At $\mathcal{T}_0 = 0$, Eq. (14) becomes

$$f_0(v) = \delta(v). \tag{15}$$

The odd moments of the ϵ distribution are zero, while the even moments are given by

$$\langle v^{2m}\rangle = \sum_{k=0}^{m} \frac{(2m)!\,\epsilon^k \mathcal{T}_0^{m-k}}{(m-k)!(2k)!\,2^{m-k}}. \tag{16}$$

The observation of any departure from Maxwellian behavior of cumulants of higher order than the kurtosis is made difficult because higher than quadratic powers of ϵ are involved. Using Eq. (16) in Eqs. (4) and (6) gives

$$\epsilon = \mathcal{T} - \mathcal{T}_0 = (-\tfrac{1}{2}\mathcal{C})^{1/2}, \tag{17}$$

thus relating the temperature rise and the kurtosis to the parameter ϵ in the ϵ distribution. $\mathcal{C}$ is the time and spatial average of $\mathcal{C}_n(t)$ behind the shock front. For strong shocks ($\alpha\nu > 1$, $\epsilon > 0$), the kurtosis is nonzero and there is no thermalization accompanying the temperature rise. We wish to emphasize that conclusions drawn from one-dimensional systems regarding thermalization are not likely to be applicable in two and three dimensions, where the thermalization process involves coupling to transverse modes that are unavailable

in one-dimensional chains. Nevertheless, we feel that simple one-dimensional systems are worth studying even if only to compare with the physics of higher-dimensional systems.

The close agreement of the two parts of Eq. (17) is a test of the validity of the ϵ distribution, as is seen in Table I. We observe an interesting paradox as shock strength increases: even though the fractional thermal shock thickness decreases, the final velocity distribution departs farther and farther from Gaussian. Thus, the speed with which the temperature reaches its final value behind the shock does not necessarily tell whether thermal equilibrium has been achieved. Typical temperature and kurtosis profiles are shown in Figs. 2 and 3.

Additional evidence for the validity of the nonequilibrium ϵ distribution is presented in Table II. Results by other investigators[2] for a shock of strength $\alpha\nu = 3$ in a Morse chain at $\mathcal{T}_0 = 0.25$ were examined and the temperature and kurtosis compared with our own calculation for the same initial conditions. Our initial temperature was set up to

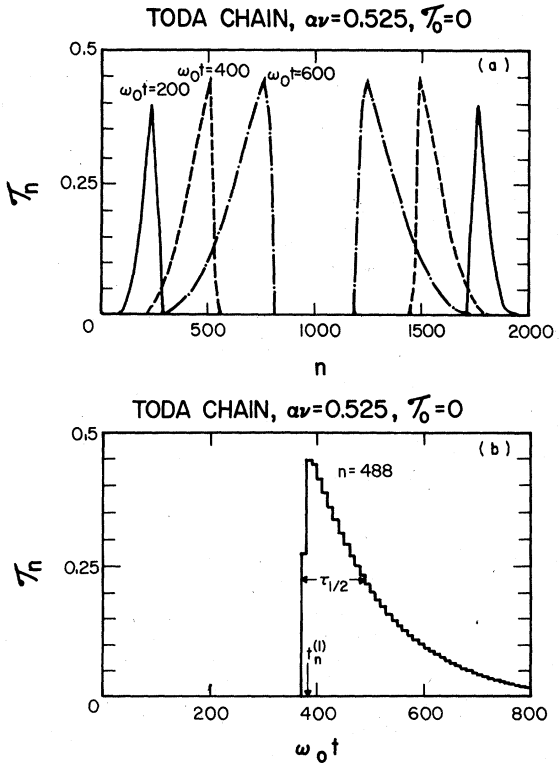

FIG. 2. Reduced temperature $\mathcal{T}_n$ [see Eq. (4)] in the Toda chain ($\alpha\nu = 0.525$, $\mathcal{T}_0 = 0$). (a) $\mathcal{T}_n$ vs particle number n at times $\omega_0 t = 200$, solid line; $\omega_0 t = 400$, dashed line; and $\omega_0 t = 600$, dot-dashed line. (b) $\mathcal{T}_n$ for $n = 488$ vs $\omega_0 t$; the thermal relaxation time $\tau_{1/2}$ is shown as well as the initial peak response time $t_n^{(1)}$.

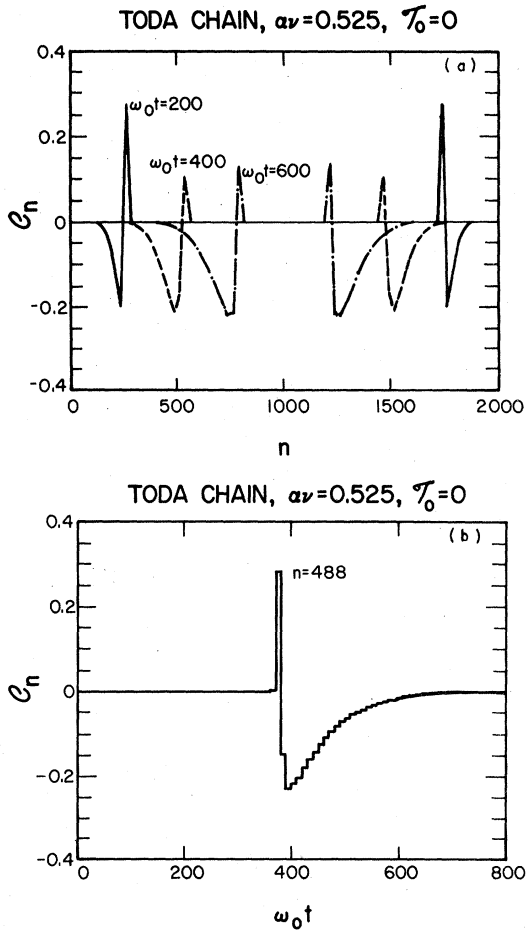

FIG. 3. Reduced kurtosis $\mathcal{C}_n$ [see Eq. (6)] in the Toda chain ($\alpha\nu = 0.525$, $\mathcal{T}_0 = 0$). (a) $\mathcal{C}_n$ vs particle number n at times $\omega_0 t = 200$, solid line; $\omega_0 t = 400$, dashed line; and $\omega_0 t = 600$, dot-dashed line. (b) $\mathcal{C}_n$ for $n = 488$ vs $\omega_0 t$.

be the same as theirs, but owing to the high anharmonicity and temperature combination, the resulting value came out 10% higher. Nevertheless, the agreement between our calculation and theirs is excellent. In both cases, the kurtosis is five standard deviations away from zero, the Maxwellian (equilibrium) value. Thus, even though the velocity distribution function does indeed *qualitatively resemble* an equilibrium distribution,[2] it is most definitely not.

It should be pointed out that the combination of shock strength $\alpha\nu = 3$ and initial temperature $\mathcal{T}_0 = 0.25$, such as in the above pair of calculations, is quite out of the ordinary, contrary to the suggestion of other workers.[2] For a weak shock in a metal such as iron (atomic weight ~60 g/mole) initially at room temperature (~300 K) the particle velocity would be ~0.4 km/sec (pressure ~200 kbars), which for iron means $\nu \sim 0.1$ since $c_0 \sim 4$

TABLE II. Comparison of the temperature and kurtosis for shock-wave calculations in the Morse chain, $\alpha\nu = 3.0$.

Investigators	$\mathcal{T}_0$	$\mathcal{C}$	$\mathcal{T} - \mathcal{T}_0$	$(-\frac{1}{2}C)^{1/2}$
Batteh and Powell[a]	0.250	−0.331	0.441	0.407
This work	0.281	−0.315±0.067	0.435	0.397

[a] Calculated from their Fig. 7 (Ref. 2).

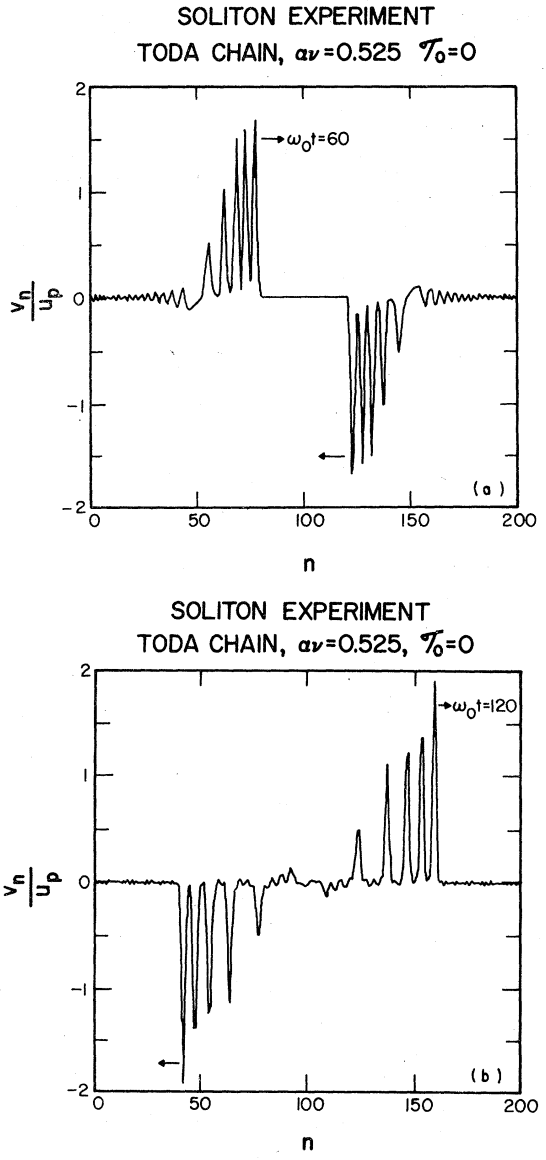

FIG. 4. (a) Velocity profile v_n/u_p vs particle number n at time $\omega_0 t = 60$ for a solition experiment in the Toda chain ($\alpha\nu = 0.525$, $\mathcal{T}_0 = 0$). The periodic length of the system shrank from time $t = 0$ to $\omega_0 t = 10$. (b) Velocity profile at time $\omega_0 t = 120$ after the first collision of the wave trains in the middle of the system.

km/sec; we then find that $\mathcal{T}_0 \sim 0.25$. For a three-dimensional crystal where atoms interact with their nearest neighbors via a pair potential, the anharmonicity α can be related to the pressure derivative of the bulk modulus B: $\alpha = 3(dB/dP - 1)/2$. For most metals, α ranges from 4 to 8, with 7 being the typical value.[3] For example, Johnson's bcc iron potential[4] has been found to correlate a wide variety of experimental data and, when used in three-dimensional molecular dynamics shock-wave calculations,[5] successfully reproduces experimental Hugoniot data for iron; the Johnson potential anharmonicity is $\alpha \sim 6$. Thus a reasonable set of parameters would be $\alpha \sim 6$, $\nu \sim 0.1$, $\alpha\nu \sim 0.6$, and $\mathcal{T}_0 \sim 0.25$. The choice of $\alpha\nu = 3$ and $\mathcal{T}_0 = 0.25$, however, implies a cubic anharmonicity coefficient of $\alpha \sim 30$, an enormous value even when compared to solid argon with $\alpha = 10.5$ (the Lennard-Jones 6–12 value[1]), which represents the upper range of anharmonicity.[3]

Finally, we have performed an experiment to generate what qualitatively resemble solitons in Toda chains by means of shock waves. Very simply, we run the shrinking periodic boundary condition scheme until a number of peaks (incipient "solitons") are formed, and then continue the calculation but with no further shrinkage of the system, so that the shock waves (left and right) are no longer supported. The two wave trains then rush toward each other, as is shown in Fig. 4(a) for $\alpha\nu = 0.525$ and $\mathcal{T}_0 = 0$, v_n vs n at $\omega_0 t = 60$. They collide in the middle (particle $n = 100$), pass through each other, and emerge essentially unchanged [see Fig. 4(b) for $\omega_0 t = 120$]. Meanwhile, each of the peaks separates from the others, the ones with larger amplitudes traveling faster (positive to the right, negative to the left). In addition, smaller-amplitude oscillations ("dreck") trail behind, while the main wave trains collide alternately at the periodic boundaries and at the middle, continuing indefinitely the process of propagation, collisions, and separation of peaks.[6] When another experiment is run at higher shock strength, $\alpha\nu = 5.25$ (at $\mathcal{T}_0 = 0$), less of the small-amplitude vibrations appear and the main peaks

(solitons) take significantly longer to separate since their amplitudes are much closer. In the hard-rod limit the small-amplitude oscillations disappear entirely and the wave train consists only of large-amplitude, closely spaced solitons. One can then speculate that the soliton formalism developed to date[7] may be difficult to apply to the shock-wave problem because of the interaction of so many closely spaced, nearly-equal-amplitude waves.

ACKNOWLEDGMENTS

This work was supported by the U. S. Department of Energy. We would like to thank H. Flashka for useful discussions and for sending us results prior to publication. One of us (R. G. P.) would like to thank the Los Alamos Scientific Laboratory for a graduate research assistantship.

---

[1]B. L. Holian and G. K. Straub, Phys. Rev. B 18, 1593 (1978).
[2]J. H. Batteh and J. D. Powell, J. Appl. Phys. 49, 3933 (1978).
[3]D. C. Wallace, *Thermodynamics of Crystals* (Wiley, New York, 1972), p. 355.
[4]R. A. Johnson, Phys. Rev. 134, A1329 (1964).
[5]B. L. Holian and G. K. Straub (unpublished).
[6]Figures 4(a) and 4(b) are two frames of a movie of the soliton experiment. The slight discrepancies in peak heights between these two frames arise from oscillations in the soliton pulses due to the discreteness of the Toda chain. The movie shows more clearly that the peaks oscillate steadily about a constant height.
[7]M. Toda, Phys. Rep. 18, 1 (1975), and references cited therein.